



# Estimation of water quality parameters using Landsat 8 images: application to Playa Colorada Bay, Sinaloa, Mexico

Luis Carlos González-Márquez<sup>1</sup> · Franklin M. Torres-Bejarano<sup>2</sup>  · Clemente Rodríguez-Cuevas<sup>3</sup> · Ana Carolina Torregroza-Espinosa<sup>4</sup> · Jorge Antonio Sandoval-Romero<sup>1</sup>

Received: 27 February 2017 / Accepted: 18 March 2018 / Published online: 26 March 2018  
© Società Italiana di Fotogrammetria e Topografia (SIFET) 2018

## Abstract

In this study, empirical models were generated to estimate water quality parameters, with the objective of showing the benefits of the satellite remote sensing application in the characterization of coastal waters. The study area was Playa Colorada Bay, located in the northwest of Mexico, in the eastern part of the Gulf of California. In two seasons of the year, on-site and laboratory characterizations were carried out to determine the spatial and temporal variation of phosphates (PO<sub>4</sub>), electrical conductivity (EC), total suspended solids (TSS), turbidity, and pH of water. Samplings were selected to match Landsat 8 satellite overpass in the study area. Radiometric and atmospheric corrections were applied to the images, prior to the generation of the models. The models were generated using the linear regression technique of successive steps; water quality parameters and their logarithms were used as dependent variables, and as independent variables were used corrected reflectance values of Landsat images. The results showed that the concentration of PO<sub>4</sub> in the analyzed water samples were higher than those recommended in the Mexican ecological criteria of water quality, to protect the aquatic life of marine water in coastal areas. In autumn, PO<sub>4</sub> was correlated with turbidity, *T*, pH, and TSS. The highest correlation coefficients were presented by TSS with PO<sub>4</sub> ( $r = -0.979$ ) and pH ( $r = 0.958$ ). The water quality models that were generated had coefficients of determination ( $R^2$ ) in the range of 0.637 to 0.955 and show the viability of the application of Landsat 8 images in the characterization of water quality parameters in Playa Colorada Bay. Models allowed the estimation of the distribution of water quality parameters over the whole bay instead of only at the sampling stations, favoring a better understanding of their spatial distribution.

**Keywords** Water pollution · Remote sensing · Eutrophication · Statistical models

## Introduction

Playa Colorada Bay is part of the lagoon system Laguna Playa Colorada - Santa María La Reforma, declared Ramsar site since 2004. This system is considered one of the most

significant areas on the Pacific coast of Mexico, being the habitat of more than 600 species, including birds, fish, amphibians, reptiles, and mammals, as well as home of resources that are exploited in it (Lyle Fritch 2003). Nevertheless, Playa Colorada Bay receives discharges from agricultural wastewater drainage systems from irrigation districts (DR) 063 and 074, untreated municipal sewage, and sewage from aquaculture farms. González-Márquez et al. (2014) reported that El Burrión collector drain, one of the main drains discharging into the bay, discharged around 0.06 and 0.71 tons of PO<sub>4</sub>-P monthly from November 2012 to July 2013. December 2012 and July 2013 generated the highest and lowest load of PO<sub>4</sub>-P, respectively. The months that presented the highest loads of PO<sub>4</sub>-P coincide with the agricultural cycle, showing the effect that this activity has on the collector drain water quality. Another economic activity affecting the water quality of agricultural drainage systems is aquaculture, as shrimp farms within the area of influence of the bay discharge their

✉ Franklin M. Torres-Bejarano  
franklintorres@correo.unicordoba.edu.co

<sup>1</sup> Department of Engineering and Technology, Universidad de Occidente, Unidad Guasave, Sinaloa, México

<sup>2</sup> Department of Environmental Engineering, Universidad de Córdoba, Montería, Colombia

<sup>3</sup> Faculty of Engineering, Universidad Autónoma de San Luis Potosí, San Luis Potosí, México

<sup>4</sup> Faculty of Engineering, Universidad de la Costa, Barranquilla, Colombia

wastewater into those systems. March is the beginning of the shrimps sowing and the harvests begin at the end of May, which finishes generally at the end of October and at the beginning of November.

Monitoring water quality may have different objectives. However, the main concerns are related to human and ecosystems health, as well as the effect it may have on economic activities that depend on it. Based on the fact that optical properties of water can be altered by variations in the concentration of parameters related to its quality (Pavelsky and Smith 2009) and that there is no restriction on the production and use of Landsat satellite images, the literature presents an increasing number of research to generate empirical models and estimate water quality parameters using the relationship between on-site and laboratory measurements with reflectance values captured in satellite images (González-Márquez et al. 2018; Bonansea et al. 2015; El Saadi et al. 2014; Harvey et al. 2015; Khattab and Merkel 2013; Lim and Choi 2015; Theologou et al. 2015; Zheng et al. 2015). In coastal waters, the most commonly used models are the empirical ones. Models that are based on the statistical relationship between the concentration of measured water quality parameters and spectral values captured using remote sensing techniques. Empirical models generated with linear regression techniques often present reliable results when applied on sites where they were generated. However, their accuracy decreases when applied to other water bodies, due to the changing site-to-site nature of the components of coastal and continental waters (Chang et al. 2014).

The objective of this research was to generate empirical water quality models to show the viability of the application of satellite remote sensing in the characterization of coastal waters in northwest Mexico. Models generated using the relationship between the concentration of  $\text{PO}_4$ , EC, TSS, turbidity, and the bay's water pH, evaluated through conventional techniques, and the reflectance recorded in Landsat 8 images.

## Study area

Playa Colorada Bay is located at latitude  $25^\circ 13' 30''$  N and longitude  $-108^\circ 21' 30''$  W, south of the municipalities of Guasave and Angostura, in the state of Sinaloa, Mexico (Fig. 1). The climate is tropical dry, with rains from June to October (Lyle Fritch 2003). In the period from 1962 to 2011, the annual average temperature was  $24.1^\circ\text{C}$ , the highest temperature was  $45.5^\circ\text{C}$ , and the lowest temperature was  $-6^\circ\text{C}$ , while the average annual evaporation was 2391 mm; the months with greater precipitation are July through September. The average annual precipitation in the period was 468.8 mm (CLICOM 2016). In the bay, the main economic activities are the fishing of shrimp, chelon, crab, and clams. In its area of influence, aquaculture is developed,

mainly the culture of shrimp, and agriculture of irrigation. The two DRs located upstream of the bay are DR063, which has an area of 100,125 ha for cultivation and DR074 with an area of 40,742 ha. The agricultural cycles, spring-summer and autumn-winter, occur from the end of September through June. The wastewater generated in the agricultural area is transported through a surface drainage system, which collects municipal and aquaculture wastewater during its course and is discharged into the bay.

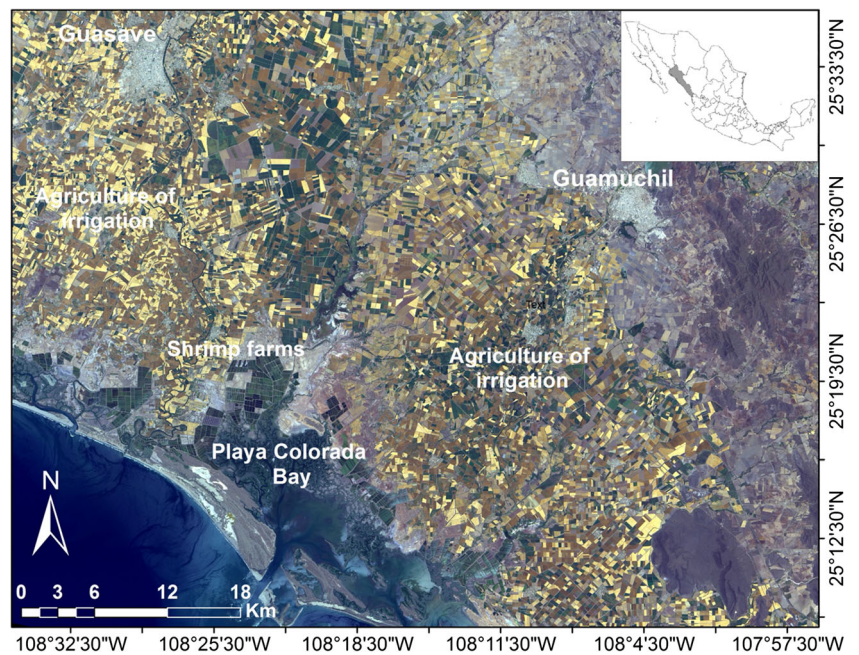
## Materials and methods

### Sampling and analysis of water quality parameters

Four sampling campaigns were conducted in the months of December 2014, May and December 2015, and June 2016. Samplings were carried out to demonstrate the effect of agricultural activity on the water quality of the bay, considering that the main contributions of  $\text{PO}_4$  to the bay are presented in the months of December and July (González-Márquez et al. 2014), these months coincide with the beginning and end of agricultural cycles in the study area. Seven to 18 sampling sites per campaign were characterized. The site location was chosen considering the distribution over the whole water surface of the bay, which could be accessed by boat and with the aim to characterize the water bay inflows and outflows. Sampling stations 1, 3, 4, 5, and 6 were at the northern part of the bay, on channels located in the mangrove area where wastewater from agricultural drainage systems enters; stations 2, 10, 19, and 23 were located along the coast between the mouth of the Sinaloa River and the mouth of the bay; the rest of the stations were in the interior of the bay. The station numbering was assigned according to latitude (Fig. 2). The  $T$ , EC, and pH of the water were measured on-site, through a multiparametric probe (YSI brand, Professional Plus model); the turbidity was evaluated with a portable turbidimeter (Hanna brand, model HI 93703 C).

For the analysis of  $\text{PO}_4$  and TSS, samples were collected from the first 40 cm of the water column. A 0.5 L Van Dorn bottle (brand LaMotte, model JT-1) was used. One hundred milliliters of water were filtered through  $0.45\text{-}\mu\text{m}$  nylon membranes (Millipore, HNWP); the filtered water was stored in plastic containers. Samples for TSS analysis were stored in 1-L glass containers. Prior to each sampling event, the containers were washed and rinsed with a 1:1 acidic solution, hydrochloric acid (analytical grade), and with MilliQ® water (MilliQ-Plus; resistivity  $> 18\text{ M}\Omega\text{ cm}$ ). The water samples were stored on ice and transported to the laboratory. In the filtered water samples,  $\text{PO}_4$  was analyzed before 48 h of sampling, according to the method 8048, reduction in ascorbic

**Fig. 1** Location of Playa Colorada Bay

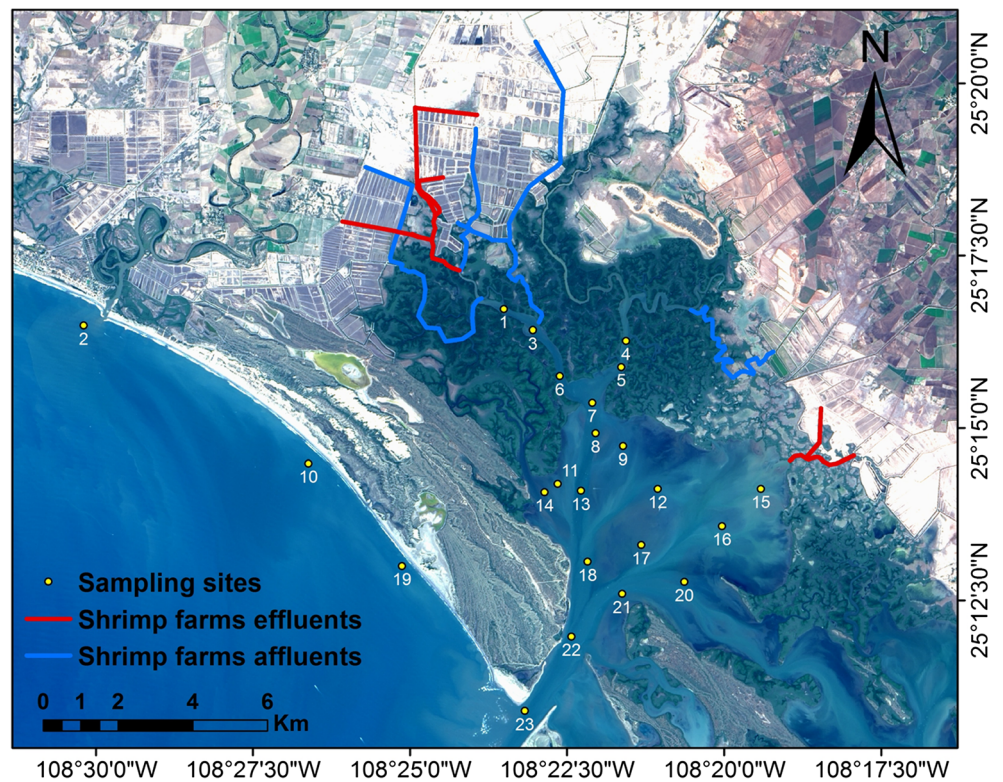


acid (HACH 2014). A VIS spectrophotometer (Hach Mark, model DR 3900) was used for PO<sub>4</sub> analysis. For the TSS analysis, 1 L of water was filtered through 1.5-µm glass fiber filters (Hach, 934-AH); the analysis was performed according to the standard methods for water and wastewater analysis (APHA-AWWA-WEF 2012). Duplicates were analyzed for quality control.

**Landsat 8 image processing**

Except for the campaign of December 2014, the sampling campaigns were matched with the day when the Landsat 8 satellite takes the image over the area where the bay is located. On-site characterization or sample collection is recommended to be done the same day of satellite image acquisition, to

**Fig. 2** Location of sampling stations



reduce errors and to obtain a better calibration of the algorithms generated to estimate water quality (Bonansea et al. 2015; Brezonik et al. 2005; Kloiber et al. 2002). In this paper, three Landsat 8 images, type GeoTIFF level 1 (path 33; row 42), were used. The images were downloaded from the US Geological Survey (USGS) database using the Global Visualization Viewer (<http://glovis.usgs.gov/>). Landsat 8 is a satellite that has two sensors, the Operational Land Imager (OLI) multispectral sensor and the Thermal Infrared Sensor (TIRS), as well as a 12-bit radiometric resolution (Roy et al. 2014). The images have 11 spectral bands, band B<sub>1</sub> (coastal/aerosol), B<sub>2</sub> (blue), B<sub>3</sub> (green), B<sub>4</sub> (red), B<sub>5</sub> (near infrared, NIR), B<sub>6</sub> and B<sub>7</sub>, (SWIR1 and SWIR2), band B<sub>9</sub> (cirrus), which all have a resolution of 30 m, and band B<sub>8</sub> (panchromatic), which has a resolution of 15 m, and bands B<sub>10</sub> and B<sub>11</sub> (TIR-1 and TIR-2), a resolution of 100 m.

Radiometric and atmospheric corrections were applied to the images. The radiometric correction was performed to transform the relative values of the pixels, or digital numbers, to absolute measurements of radiation per unit wavelength of light or to reflectance, while the atmospheric correction was performed to eliminate the atmospheric effects, and thereby transform the radiometric values into radiation or surface reflectance, so that the water quality parameters could be estimated and compared in time and space. Atmospheric correction was made applying the dark object subtraction method (Chavez 1996), which considers that in an image, some dark objects have values of reflectance close to zero; however, due to atmospheric dispersion and absorption, non-zero reflectance values are recorded in the pixels where such objects are located. These values must be subtracted from the different spectral bands of the image. The images were processed in QGIS (version 2.14), using the Semi-Automatic Classification Plugin (Congedo 2016).

### Models for estimating water quality parameters

For the determination of the statistical models, the water quality parameters and their logarithms were used as dependent variables, and as independent variables were used values of reflectance (individual band, combinations of bands, square roots, reciprocals, square, cubic, powers, sums, subtractions, logarithms, and band ratios) of the processed Landsat images. The models were generated using the linear regression technique of successive steps, using Matlab version 2015. The root mean square error (RMSE) and the determination coefficients ( $R^2$ ) were used to evaluate precision of the fit of the regression model to water quality parameters.

### Statistical analysis

The differences between the evaluated parameters in sampling I and sampling II were evaluated statistically by Student's  $t$  tests ( $P < 0.05$ ). Correlation analysis was performed using the

Pearson correlation coefficient ( $r$ ), a coefficient that can have values between  $-1$  and  $+1$ , passing through zero. Values close to  $-1$  indicate that the variables are inversely associated strongly, while values close to  $+1$  indicate that the variables have a strong direct relationship. Values close to zero are not associated (Berthouex and Brown 2002). The Pearson correlation coefficient formula is defined as follows (Eq. 1):

$$r = \frac{\sum_{i=1}^n (x_i - \bar{x})(y_i - \bar{y})}{\sqrt{\sum_{i=1}^n (x_i - \bar{x})^2 \sum_{i=1}^n (y_i - \bar{y})^2}} \quad (1)$$

where,  $x_i$  and  $y_i$  are concentrations of different water quality parameter;  $\bar{x}$  and  $\bar{y}$  are the mean concentrations of the water quality parameters. It was considered that the parameters are related when the level of significance is less than 0.05 ( $P < 0.05$ ). The objective of the correlation analysis was to identify if the parameters not optically active were related to those that do are, and therefore to know the potential to be evaluated through models generated from Landsat 8 images.

## Results

### On-site water quality results

In the autumn of 2014 and 2015, PO<sub>4</sub> concentrations in the bay water samples were higher than those recommended in the Mexican ecological criteria of water quality for the protection of aquatic life in marine waters in coastal areas, PO<sub>4</sub> = 0.002 mg/L (DOF 1989). The maximum, average and minimum concentrations of PO<sub>4</sub> were 0.27, 0.131, and 0.05 mg/L, respectively (Table 1). In spring, the concentrations were also higher than those recommended in the ecological criteria of water quality. The maximum, average, and minimum concentrations of PO<sub>4</sub> were 0.20, 0.08, and 0.05 mg/L, respectively (Table 2). The concentration of PO<sub>4</sub> presented a significant difference ( $P < 0.05$ ) in the samplings performed in autumn and spring, showing higher concentrations in autumn. The average concentrations of PO<sub>4</sub> in autumn were 1.6 higher than in spring. The average water temperature in autumn and spring was 23.3 and 28.3 °C, respectively. In general, EC, TSS, and water turbidity presented a similar attendance, with values higher in spring than in autumn. Parameters that were not evaluated were represented with ND in the cells of Tables 1 and 2.

### Correlation between water quality parameters

In December of 2014, there were no significant correlations between the water quality parameters evaluated in the bay, a

**Table 1** Average evaluation results of water quality parameters in Playa Colorada Bay, in autumn 2014 and 2015

Station	<i>T</i> (°C)	PO <sub>4</sub> (mg/L)	TSS (mg/L)	Turbidity (NTU)	pH	EC (mS/cm)
1	22.5	0.27	24.7	9.0	7.98	46.38
2	23.0	0.25	ND	7.7	8.30	54.78
3	22.8	0.24	28.6	6.5	8.02	46.75
4	22.4	0.24	24.6	7.2	8.00	42.05
5	22.4	0.20	40.9	7.2	8.03	46.53
6	22.7	0.17	ND	4.5	8.09	48.13
7	23.2	0.10	57.9	5.1	8.08	49.52
8	22.9	0.13	ND	3.8	8.14	47.39
9	ND	ND	ND	ND	ND	ND
10	22.9	0.06	ND	3.8	8.35	51.52
11	23.6	0.10	ND	7.7	8.24	49.41
12	24.1	0.08	ND	ND	8.10	50.74
13	23.8	0.13	ND	3.1	8.11	48.27
14	ND	ND	ND	ND	ND	ND
15	24.5	0.10	ND	ND	7.99	49.38
16	23.4	0.11	ND	7.0	8.41	47.56
17	23.1	0.08	ND	4.6	8.37	48.95
18	23.4	0.10	ND	1.2	8.18	48.89
19	23.2	0.09	ND	3.2	8.39	51.61
20	23.5	0.06	ND	2.3	8.23	49.94
21	24.4	0.05	ND	4.7	8.40	49.73
22	ND	ND	ND	ND	ND	ND
23	24.2	0.08	ND	4.9	8.23	52.06

ND no data

non-shaded region of Table 3. In the shaded region of Table 3, the coefficients of correlation between parameters evaluated in December 2015 are presented. In that month, significant correlations were presented. The concentration of PO<sub>4</sub> was correlated ( $P < 0.01$ ) with  $T$  ( $n = 18$ ), pH ( $n = 17$ ), turbidity ( $n = 18$ ), and TSS ( $n = 5$ ). The pH of the water also presented correlations with  $T$  ( $n = 17$ ) ( $P < 0.01$ ), turbidity ( $n = 17$ ) ( $P < 0.05$ ) and TSS ( $n = 5$ ) ( $P < 0.05$ ), as well as with EC ( $n = 17$ ) ( $P < 0.01$ ). The strongest correlations were presented by TSS with pH ( $r = 0.958$ ) and with PO<sub>4</sub> ( $r = -0.979$ ). In spring, different correlations were presented to those of autumn (Table 4). In the unshaded region of Table 4, it can be observed that in May of 2015, only pH and EC were correlated ( $n = 15$ ), presenting a positive and significant correlation ( $P < 0.01$ ). In June of 2016, the shaded region of Table 4, the water temperature presented positive correlations with turbidity ( $n = 15$ ) and with TSS ( $n = 13$ ), while TSS was positively related to turbidity ( $n = 13$ ).

### Water quality models

Through linear regression technique of successive steps, satisfactory models were obtained to estimate PO<sub>4</sub>, EC, TSS, turbidity, and pH in bay water. The generated models ( $P <$

0.05), as well as the  $R^2$  and the RMSE are presented in Table 5. In spring 2015 and 2016, the PO<sub>4</sub> concentration presented  $R^2$  of 0.755 and 0.867, respectively, being significantly related to bands B<sub>5</sub>, B<sub>6</sub>, and B<sub>7</sub>, in both years (Fig. 3). PO<sub>4</sub> is not an optically active molecule, so it cannot be measured directly through optical instruments. However, because it can be correlated with other water constituents which are optically active (Gholizadeh et al. 2016; C. Wu et al. 2010), it was possible to generate models to estimate their concentration in the bay. Nevertheless, in spring, PO<sub>4</sub> did not present a positive correlation with any of the parameters evaluated in the bay. Probably, optically active parameters that were not evaluated, and that could have presented correlation with PO<sub>4</sub>, were responsible for the high  $R^2$  of the generated models.

The concentration of TSS was related to bands B<sub>1</sub>, B<sub>2</sub>, and B<sub>3</sub> in May of 2015 and bands B<sub>5</sub> and B<sub>6</sub> in June of 2016, whereas in December of the same year, it was only related to B<sub>6</sub>. Different authors have reported that reflectivity in the range of 760 to 1100 nm plays an important role in the characterization of TSS (Ma and Dai 2005; Zheng et al. 2015). Also, TSS has been reported to be related to bands B<sub>2</sub>, B<sub>3</sub>, and B<sub>8</sub> (Zhang et al. 2015), coinciding with the relationships found in this research. Turbidity was related to bands B<sub>2</sub> and B<sub>4</sub> in May of

**Table 2** Average evaluation results of water quality parameters in Playa Colorada Bay, in spring 2015 and 2016

Station	T (°C)	PO <sub>4</sub> (mg/L)	TSS (mg/L)	Turbidity (NTU)	pH	EC (mS/cm)
1	27.70	ND	60.70	9.1	7.87	50.01
2	27.55	0.07	58.70	8.2	7.95	51.82
3	27.75	0.06	60.30	7.8	7.90	50.63
4	29.60	0.07	49.40	4.7	7.53	52.61
5	28.55	0.09	50.47	2.2	7.79	45.09
6	28.05	0.07	34.64	7.3	7.88	50.04
7	28.90	0.11	51.52	4.3	7.84	50.27
8	29.10	0.05	45.40	5.7	7.72	53.90
9	27.10	0.07	40.00	6.4	8.19	50.02
10	ND	ND	ND	ND	ND	ND
11	30.40	0.10	ND	7.0	7.67	54.29
12	28.50	0.06	ND	2.7	8.15	51.54
13	28.70	0.08	41.48	9.3	7.95	51.63
14	27.40	0.12	47.35	34.7	8.16	48.15
15	28.70	0.07	134.55	64.5	8.17	51.12
16	29.35	0.07	58.80	17.0	7.95	53.00
17	28.90	0.09	40.60	8.4	7.94	52.65
18	26.70	0.07	53.33	ND	8.17	51.75
19	28.80	0.08	37.80	2.6	7.82	52.39
20	27.60	0.11	47.10	1.7	8.17	52.07
21	29.40	0.06	41.40	4.7	7.78	53.13
22	26.70	0.11	ND	ND	8.11	52.01
23	27.75	ND	ND	1.1	7.95	52.37

ND no data

2015, with B<sub>3</sub>, B<sub>4</sub>, B<sub>5</sub>, and B<sub>6</sub> in June 2016. While in December 2015, it was related to bands B<sub>1</sub>, B<sub>4</sub>, B<sub>5</sub>, and B<sub>6</sub>. Previous studies indicate that turbid waters have high reflectance in bands B<sub>4</sub> and B<sub>5</sub> (Kumar et al. 2016; Khattab and Merkel 2013; Wu et al. 2009), being in line with what was found in the present investigation. However, it was also related to other bands, which may be because water of the bay presented a great variability in the composition of its constituents, presenting turbid waters in the north part and little turbid or transparent in the south part. TSS was associated with bands B<sub>1</sub>, B<sub>2</sub>, and B<sub>3</sub> in May 2015, with B<sub>5</sub> and B<sub>6</sub> in June 2016, and with

B<sub>6</sub> in December 2015. Considering that TSS may be associated with the presence of phytoplankton in the bay, the bands that would relate would be B<sub>4</sub> and B<sub>5</sub> bands; however, as well as turbidity, the variability of water composition causes it to be related to other bands of the electromagnetic spectrum (Yacobi et al. 2011); Bands B<sub>2</sub> and B<sub>3</sub> generally yield good results when estimating chlorophyll *a* (Yunus et al. 2015). EC was associated with bands B<sub>1</sub> and B<sub>5</sub> in May 2015 with B<sub>1</sub>, B<sub>2</sub>, B<sub>3</sub>, B<sub>5</sub>, and B<sub>6</sub> in June 2016 and with B<sub>1</sub>, B<sub>3</sub>, B<sub>6</sub>, and B<sub>7</sub> in December 2015. The increase in water salinity causes changes in the amount of reflected radiation in the visible and infrared

**Table 3** Linear correlation of water quality parameters. The unshaded data correspond to autumn, December of 2014 and the shaded ones to December of 2015

	T	EC	pH	PO <sub>4</sub>	Turbidity	TSS
T	1	0.263	0.140	0.697	ND	ND
EC	0.439	1	0.591	-0.205	ND	ND
pH	<b>0.672**</b>	<b>0.664**</b>	1	-0.391	ND	ND
PO <sub>4</sub>	<b>-0.613**</b>	-0.386	<b>-0.790**</b>	1	ND	ND
Turbidity	-0.157	-0.237	<b>-0.494*</b>	<b>0.656**</b>	1	ND
TSS	0.561	0.553	<b>0.958*</b>	<b>-0.979**</b>	-0.772	1

ND no data

\*The correlation is significant at 0.05

\*\*The correlation is significant at the level 0.01

**Table 4** Linear correlation of water quality parameters. The unshaded data correspond to spring, May of 2015 and the shaded ones to June of 2016

	T	EC	pH	PO <sub>4</sub>	Turbidity	TSS
T	1	0.123	0.178	0.125	0.484	0.418
EC	0.061	1	<b>0.726**</b>	0.216	0.096	0.129
pH	-0.288	0.331	1	0.305	0.403	0.045
PO <sub>4</sub>	0.418	0.124	-0.142	1	0.084	0.154
Turbidity	<b>0.599*</b>	0.175	-0.254	0.007	1	0.441
TSS	<b>0.807**</b>	-0.136	-0.259	-0.114	<b>0.748**</b>	1

\*The correlation is significant at 0.05

\*\*The correlation is significant at the level 0.01

spectrum bands (Khattab and Merkel 2013; Theologou et al. 2015). Regarding pH, it was related to bands B<sub>1</sub>, B<sub>3</sub>, B<sub>4</sub>, and B<sub>5</sub> in May 2015 with R<sup>2</sup> of 0.637, being the lowest relation between water quality parameters and spectral bands. In June of 2016, it was related to B<sub>2</sub>, B<sub>3</sub>, and B<sub>5</sub> and in December 2015, with B<sub>1</sub> and B<sub>5</sub>. pH is the negative logarithm of H<sup>+</sup> ion concentration and has been associated with short wave infrared bands (Theologou et al. 2015).

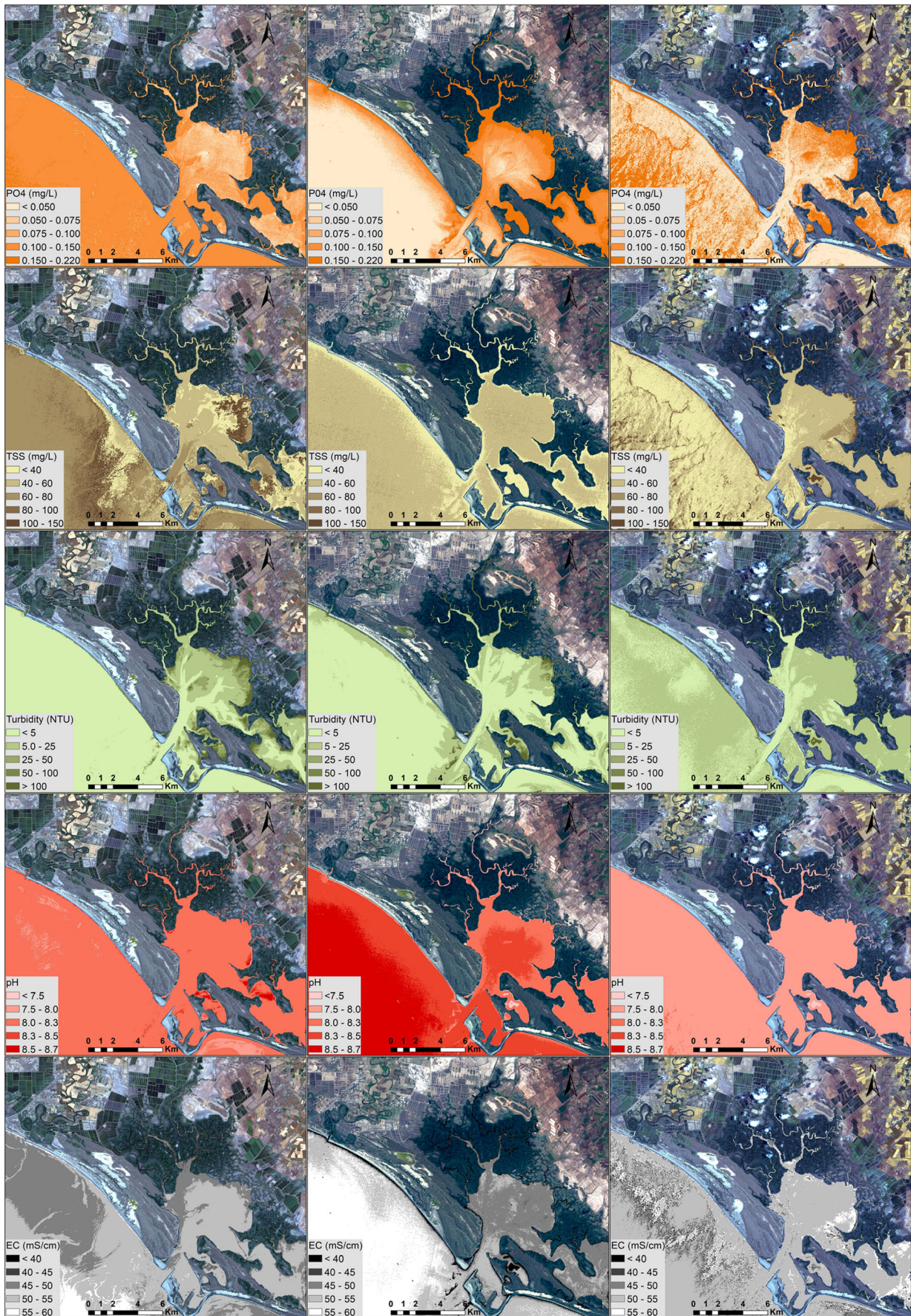
### Spatial distribution of water quality parameters

The application of the generated models to the satellite images is allowed to generate maps of spatial variation of PO<sub>4</sub>, EC, TSS, turbidity, and pH in Playa Colorada Bay (Fig. 3). The highest concentrations of PO<sub>4</sub> occur in

the areas closest to the coast, mainly in the northeastern part of the bay and in their tributaries. The highest concentration of PO<sub>4</sub> was presented in December of 2015, evidencing the contribution of PO<sub>4</sub> from the agricultural drainage systems to the bay, as described by González-Márquez et al. (2014). In May of 2015, the TSS concentration also showed higher values in the northeast part of the bay, with concentrations higher than 100 mg/L. In December of the same year, the concentrations of TSS were less than 40 mg/L. However, in June of 2016, concentrations between 60 and 100 mg/L of TSS were present in the northeast part of the bay. The turbidity of the water also presented murkier waters in the northeast part of the bay. In May of 2015, the highest values of turbidity were presented and in July, they presented clearer waters, with turbidity values lower than 25 NTU in most of the

**Table 5** Models for estimating water quality parameters, generated from Landsat 8 images

Parameters and equations	R <sup>2</sup>	RMSE
Spring of 2015		
Log (PO <sub>4</sub> ) = -0.95224 + (0.00010714*( $\frac{1}{B5^2}$ )) + (-0.0000018412*( $\frac{1}{B6^3}$ )) + (0.00000000090663*( $\frac{1}{B7^5}$ ))	0.755	0.060
TSS = 45.209 + 7.5403 * ((B1 - B3)/(B1 - B2))	0.818	13.600
Log(Turbidity + 15) = 1.4562 + 42.333 * (B4 - B2) + 1527.6 * (B4 - B2) <sup>2</sup>	0.784	0.108
pH = 8.1391 + 5.698 * (B1 - B4) - 0.3226 * ((B1 - B3)/(B1 - B5))	0.637	0.038
EC = 62.856 - 0.77356*( $\frac{1}{B1}$ ) + 0.0014973*( $\frac{1}{B5^2}$ )	0.694	2.130
Autumn of 2015		
Log (PO <sub>4</sub> ) = -0.64983 - 0.0000000000025586*( $\frac{1}{B5^7}$ )	0.660	0.159
TSS = 276.44 - 18960 * B6	0.955	3.480
Log (Turbidity) = - 10.399 + 78.55 * (B4 + B5) + 12.37 * ((B1 - B6)/(B1 + B4))	0.777	0.110
pH = 7.4059 + 0.25376*( $\frac{B1}{B5}$ )	0.947	0.037
EC = - 682.74 + 1399.7 * B1 - 484.9 * B3 + 57161 * B6 + 59602 * B7 - 5079300 * B6 * B7	0.849	1.250
Spring of 2016		
Log(PO <sub>4</sub> ) = - 14.383 + 107.32 * Log(B5) - 36.249 * Log(B6) - 82.972 * Log(B7) + 33.252 * (Log(B5)) <sup>2</sup> - 34.867 * (Log(B7)) <sup>2</sup>	0.867	0.063
Log(TSS) = 5.7888 + (15.864 * Log(B5)) + (-9.6808 * Log(B6)) + (5.1006 * (Log(B5)) <sup>2</sup> ) + (-2.8631 * (Log(B6)) <sup>2</sup> )	0.853	0.029
Log(Turbidity + 15) = 1.1093 + 8.6654 * B3 - 5.3409 * B4 + 18.239 * B5 - 21.055 * B6	0.778	0.025
pH = 8.4392 + 2.2981 * Log(B2) - 1.3567 * Log(B3) - 0.37299 * Log(B5)	0.884	0.033
EC = 52.412 + 157.56 * (B1 - B2) + 0.0044809 * (1/(B1 - B3)) - 0.36922 * ((B1 - B6)/(B1 - B3)) - 2.2498 * ((B2 - B3)/(B2 - B5))	0.884	0.445





◀ **Fig. 3** Concentrations of water quality parameters, estimated through models generated from Landsat 8 images (Left: in May 2015; Center: December 2015; Right: June 2016)

water mirror. The pH had the lowest values in May 2015 and June 2016, while the EC presented an inverse behavior, with lower values in December 2015.

## Discussion

### Water quality

Anthropogenic activities in the area of influence of Playa Colorada Bay generate wastewater which is discharged in the bay without previous treatment, affecting the quality of its water. The results of the present study coincide with those reported on the higher concentrations of  $\text{PO}_4$  in autumn than in the spring ( $P < 0.05$ ), which were reported by González-Márquez et al. (2014), evidencing the effect of wastewater from the agricultural sector on the water quality of the bay. In the spring sampling campaigns of 2015 and 2016, the shrimp harvest on aquaculture farms had already begun. During that time, discharges of untreated aquaculture and domestic wastewater, located in the bay basin, appear to be the main sources of  $\text{PO}_4$ , since there is no input of residual water from agriculture. Eighty-eight and 92% of the samples analyzed in autumn and spring, respectively, presented concentrations higher than the problematic value of phosphorus (0.02 mg/L) for eutrophication of receiving water bodies proposed by (Correll 1998); the highly unacceptable concentration of 0.1 mg/L was not exceeded in the autumn or spring. From the evaluated on-site results, it is observed that in autumn of 2015 the  $\text{PO}_4$  concentration tended to decrease as a function of the latitude of the sampling stations, indicating a possible dilution effect and/or assimilation of the compound during its stay in the bay. In spring, the average  $\text{PO}_4$  concentration did not show a tendency to decrease or increase with respect to the location of the sampling stations. This could be explained by the absence of agricultural wastewater inputs to the bay in spring, and therefore, lower  $\text{PO}_4$  loads in the tributaries, as well as lower phosphate concentrations at sea (Fig. 3) that favored the dilution process in the bay. The highest concentrations of TSS and the highest values of turbidity were present in the sampling stations closest to the tributaries of the bay, as well as the lowest values of pH and EC.

### Correlation analysis

In December 2014, there were no significant correlations between the evaluated water quality parameters, may be due to the small number of characterized sampling sites ( $n = 7$ ). Unlike what has been reported in the literature (Uusitalo

et al. 2000), where it has been found that TSS is not related to  $\text{PO}_4$ , in this study, the concentrations of  $\text{PO}_4$  evaluated in December of 2015 had a strong negative relation with the concentration of TSS (Table 3). This relationship can be explained if the TSS were constituted mainly by phytoplankton, since  $\text{PO}_4$  could be incorporated by the latter (Sosa-Avalos et al. 2013) or by dilution of  $\text{PO}_4$  in the bay, as described above. Turbidity is a measure of the clarity of water. The decrease in clarity or increase in turbidity is usually caused by suspended or dissolved solids or particles, which cause the dispersion and absorption of light in the water column. Turbidity presented a significant positive correlation with  $\text{PO}_4$  ( $P < 0.01$ ), as well as a negative relation with pH ( $P < 0.05$ ); this can be explained by the influence of the freshwater currents of the agricultural drainage systems that discharge in the bay, which influence the concentration of dissolved and suspended solids, affecting the clarity of the water of the bay and favoring the concentration of  $\text{PO}_4$ . The stations with the highest turbidity and lower pH are located in the vicinity of the tributaries of the bay, in the northern part, while in the stations closer to the sea, in the southern part, there was lower turbidity and higher pH. TSS showed a negative relation with turbidity ( $r = -0.772$ ); however, it was not significant ( $P = 0.12$ ), may be due to the small number of TSS samples analyzed. Considering that turbidity was negatively correlated with pH and positively with  $\text{PO}_4$ , as well as in most of the bay, the  $\text{PO}_4$  concentration is high, mainly in the tributaries, whereas the TSS have an inverse behavior; these correlations could support the assumption that TSS were constituted mainly by phytoplankton. As in continental and coastal waters, which are generally turbid and productive, the concentration of non-algal particles or solids is not related to the concentration of phytoplankton (Yacobi et al. 2011). Therefore, the turbidity may be controlled mainly by suspended or dissolved solids less than 1.5  $\mu\text{m}$ , which were not retained in the filters for TSS analysis. In spring 2016, TSS and turbidity once again showed a strong correlation; however, this time, it was positive and significant ( $P < 0.01$ ). This could be because in spring, a larger number of sampling stations ( $n = 13$ ) were evaluated than in autumn, since from late May shrimp farms discharge wastewater with high concentrations of TSS to the bay. Results are consistent with those reported in the literature (Pavelsky and Smith 2009), where it has been suggested that TSS is the main factor controlling water clarity.

### Water quality models

The water quality models generated in this study show the viability of Landsat 8 images application in the characterization of  $\text{PO}_4$ , EC, TSS, turbidity, and pH in Playa Colorada Bay. Models allowed the estimation of water quality parameters distribution over the whole bay instead of only at the sampling stations, favoring a better understanding of their spatial

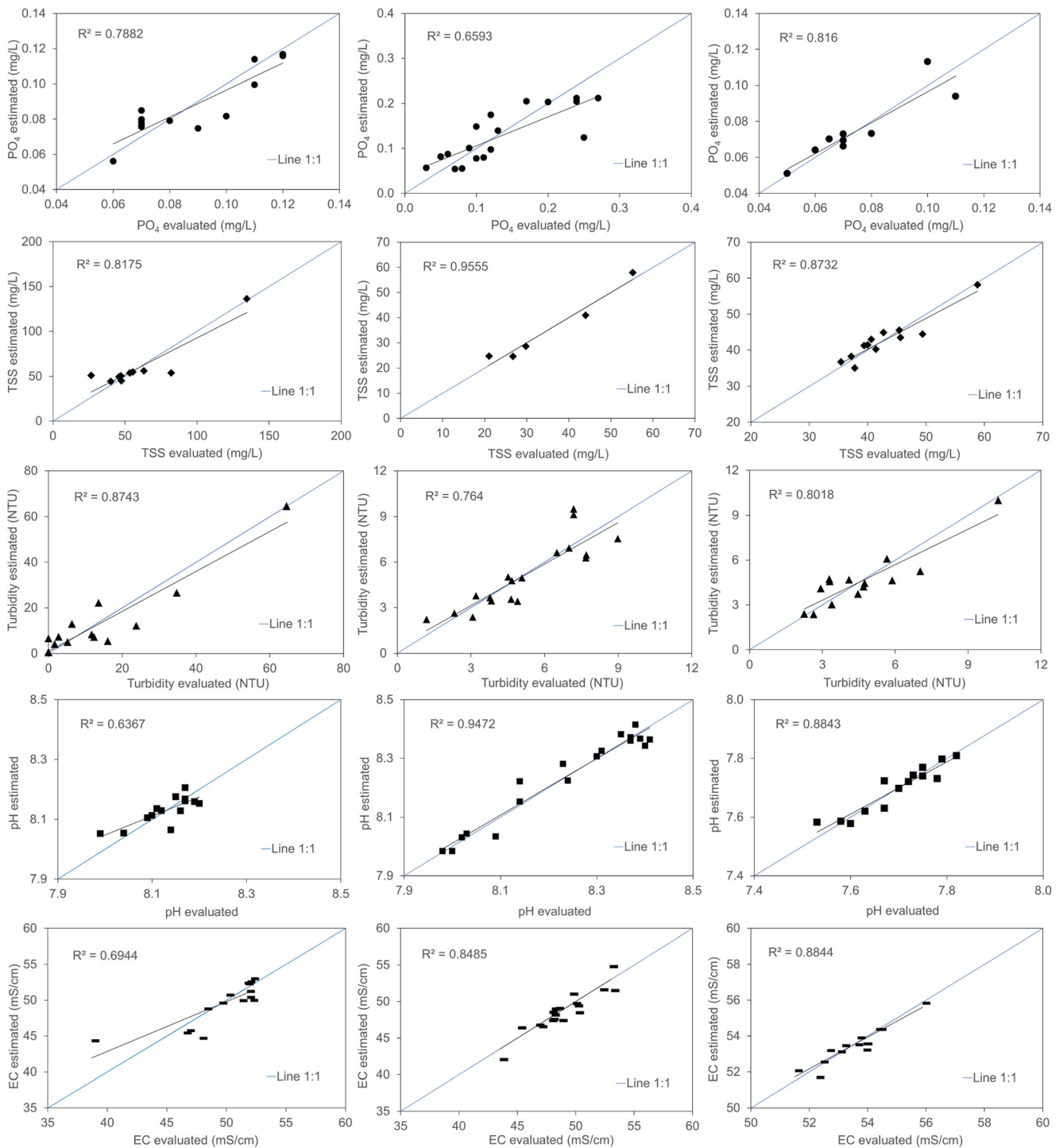


**Fig. 4** Parameters measured on-site versus estimated using Landsat 8 images (Left: in May 2015; Center: December 2015; Right: June 2016)

distribution. The reflectance of the spectral bands of Landsat 8 images and water quality parameters showed relatively high correlations ( $R^2$  ranging between 0.637 and 0.955). Models presented in Table 5 showed satisfactory results according to the RMSE and  $R^2$ . TSS presented the highest  $R^2$  value, while pH presented the lowest value, but these results show the viability of these types of models, mainly in the estimation of

water constituents which are optically active. Even when TSS, an optically active component in water, did not present correlations with all not optically active parameters, it was possible to obtain satisfactory models, since such parameters could have been related to optically active parameters that were not evaluated in this study, such as chlorophyll *a* and color of dissolved organic matter (Li et al. 2017). Figure 4 shows

graphically the relationship between water quality parameters estimated through the models and the results evaluated on-site. The seven bands of Landsat 8 contributed to the generation of water quality models. From the simplest models, PO<sub>4</sub> and TSS generated for autumn of 2015, which were generated with a single band to more complex models such as EC in the spring of 2016. However, the models generated in the present study differ from reported models in the literature (El Saadi et al. 2014; Khattab and Merkel 2013; Lim and Choi 2015), showing the need for a recurring parameterization and calibration due to the changing nature of the components of coastal waters (Yacobi et al. 2011). This is one of the main disadvantages of empirical models (Chang et al. 2014).

## Conclusions

Agricultural, aquaculture, and domestic activities in the area of influence of Playa Colorada Bay discharge wastewater to the bay without previous treatment affecting its water quality and environmental health. Between autumn and spring, the concentration of PO<sub>4</sub> presented a significant difference ( $P < 0.05$ ). The average concentrations of PO<sub>4</sub> in autumn were 1.6 times higher than in spring, showing the negative effect of agricultural effluents in the bay. PO<sub>4</sub> exceeds the recommendations established by the Mexican Ecological Criteria of water quality in most of the bay, which represents a potential negative impact on aquatic life.

The diminution in clarity or increase in turbidity is usually caused by suspended or dissolved solids or particles, which cause the dispersion and absorption of light in the water column. Turbidity presented a significant positive correlation with PO<sub>4</sub> ( $P < 0.01$ ), as well as a negative relation with pH ( $P < 0.05$ ); this can be explained by the influence of the freshwater currents of the agricultural drainage systems discharging in the bay, which influence the concentration of dissolved and suspended solids, affecting the water clarity of the bay and favoring the concentration of PO<sub>4</sub>.

The estimation of water quality parameters through satellite remote sensing techniques can complement and improve traditional methods of water characterization. The water quality models generated from Landsat 8 images and concentrations of PO<sub>4</sub>, EC, TSS, turbidity, and pH evaluated presented coefficients of determination ranging from 0.637 to 0.955, showing their potential in the estimation of water quality parameters in Playa Colorada Bay, mainly in the estimation of water constituents which are optically active. However, the models generated in this study were different in each of the evaluated seasons and differ from reported models in the literature, showing the need for a recurring parameterization and calibration due to the changing nature of the components of coastal waters.

Unlike the results obtained with the traditional methods, through the results generated with the models, more detailed patterns of the distribution of water quality parameters throughout the bay can be identified. Models allowed the estimation of the value of water quality parameters over the whole bay instead of only at the sampling stations.

The implementation of a traditional monitoring system, complemented with the application of satellite remote sensing for the estimation of parameters of water quality, could facilitate the environmental, economic, and social management of Playa Colorada Bay.

## References

- APHA-AWWA-WEF (2012) Standard methods for the examination of water and wastewater. In: E. W. Rice, R. B. Baird, A. D. Eaton, & L. S. Clesceri (Eds.) (22nd ed.). American Public Health Association, American Water Works Association, Water Environment Federation
- Berthouex PM, Brown LC (2002) Statistics for environmental engineers. Lewis Publishers, Boca Raton
- Bonanse M, Rodriguez MC, Pinotti L, Ferrero S (2015) Using multi-temporal Landsat imagery and linear mixed models for assessing water quality parameters in Río Tercero reservoir (Argentina). *Remote Sens Environ* 158:28–41. <https://doi.org/10.1016/j.rse.2014.10.032>
- Brezonik P, Menken KD, Bauer M (2005) Landsat-based remote sensing of lake water quality characteristics, including chlorophyll and colored dissolved organic matter (CDOM). *Lake Reservoir Manage* 21(4):373–382. <https://doi.org/10.1080/07438140509354442>
- Chang N-B, Imen S, Vannah B (2014) Remote sensing for monitoring surface water quality status and ecosystem state in relation to the nutrient cycle: a 40-year perspective. *Crit Rev Environ Sci Technol* 45(July 2015):140225124012009–140225124012166. <https://doi.org/10.1080/10643389.2013.829981>
- Chavez PS (1996) Image-based atmospheric corrections—revisited and improved. *Photogramm Eng Remote Sens* 62(9):1025–1036
- CLICOM. (2016). Datos climáticos diarios del CLICOM del SMN a través de su plataforma web del CICESE. Retrieved September 6, 2016, from <http://clicom-mex.cicese.mx>
- Congedo L (2016) Semi-automatic classification plugin documentation. <https://doi.org/10.13140/RG.2.2.29474.02242/1>
- Correll DL (1998) The role of phosphorus in the eutrophication of receiving waters: a review. *J Environ Qual* 27(2):261. <https://doi.org/10.2134/jeq1998.00472425002700020004x>
- DOF (1989) Criterios Ecológicos de Calidad del Agua CE- CCA-001/8. Diario Oficial de la Federación. México, 13 de diciembre de 1989. [http://www.dof.gob.mx/nota\\_detalle.php?codigo=4837548&fecha=13/12/1989](http://www.dof.gob.mx/nota_detalle.php?codigo=4837548&fecha=13/12/1989)
- El Saadi AM, Yousry MM, Jahin HS (2014) Statistical estimation of Rosetta branch water quality using multi-spectral data. *Water Sci* 28(1):18–30. <https://doi.org/10.1016/j.wsj.2014.10.001>
- Gholizadeh MH, Melesse AM, Reddi L (2016) A comprehensive review on water quality parameters estimation using remote sensing techniques. *Sensors (Basel, Switzerland)*, 16(8), 1298. doi: <https://doi.org/10.3390/s16081298>
- González-Márquez LC, Figueroa Moreno MA., Hansen Rodríguez IR, Rodríguez Gallegos HB, Trigueros Salmerón Á (2014) Fosfatos en agua de drenaje agrícola: cuenca baja del Río Sinaloa. *Ciencia Desde El Occidente*, 1(2), 19–28. Retrieved from <http://udo.mx/>

- portal/images/archivos/cienciadesdeoccidente/2016/VOL1/VOL1 No2 2015 ARTÍCULO 3.pdf
- González-Márquez LC, Torres-Bejarano FM, Torregroza-Espinosa AC, Hansen-Rodríguez IR, Rodríguez-Gallegos HB (2018) Use of LANDSAT 8 images for depth and water quality assessment of El Guájaro reservoir, Colombia. *J S Am Earth Sci* 82(March 2018): 231–238. <https://doi.org/10.1016/j.jsames.2018.01.004>
- HACH (2014) PhosVer 3 phosphate reagent powder pillows. Retrieved December 1, 2014, from <http://www.hach.com/phosver-3-phosphate-reagent-powder-pillows-10-ml-pk-100/product?id=7640196043>
- Harvey ET, Kratzer S, Philipson P (2015) Satellite-based water quality monitoring for improved spatial and temporal retrieval of chlorophyll-*a* in coastal waters. *Remote Sens Environ* 158:417–430. <https://doi.org/10.1016/j.rse.2014.11.017>
- Khatab MFO, Merkel BJ (2013) Application of Landsat 5 and Landsat 7 images data for water quality mapping in Mosul Dam Lake, Northern Iraq. *Arab J Geosci* 7(9):3557–3573. <https://doi.org/10.1007/s12517-013-1026-y>
- Kloiber SM, Brezonik PL, Olmanson LG, Bauer ME (2002) A procedure for regional lake water clarity assessment using Landsat multispectral data. *Remote Sens Environ* 82(1):38–47. [https://doi.org/10.1016/S0034-4257\(02\)00022-6](https://doi.org/10.1016/S0034-4257(02)00022-6)
- Kumar V, Sharma A, Chawla A, Bhardwaj R, Thukral AK (2016) Water quality assessment of river Beas, India, using multivariate and remote sensing techniques. *Environ Monit Assess*, 188(3):1–10. <https://doi.org/10.1007/s10661-016-5141-6>
- Li Y, Zhang Y, Shi K, Zhu G, Zhou Y, Zhang Y, Guo Y (2017) Monitoring spatiotemporal variations in nutrients in a large drinking water reservoir and their relationships with hydrological and meteorological conditions based on Landsat 8 imagery. *Sci Total Environ* 599–600: 1705–1717. <https://doi.org/10.1016/j.scitotenv.2017.05.075>
- Lim J, Choi M (2015) Assessment of water quality based on Landsat 8 operational land imager associated with human activities in Korea. *Environ Monit Assess* 187(6):1–17. <https://doi.org/10.1007/s10661-015-4616-1>
- Lyle Fritch PL (2003) Laguna Playa Colorada-Santa María La Reforma. Ficha Informativa de los Humedales de Ramsar (FIR). Mazatlán, Sinaloa. Retrieved from <https://rsis.ramsar.org/RISapp/files/RISrep/MX1340RIS.pdf>
- Ma R, Dai J (2005) Investigation of chlorophyll-*a* and total suspended matter concentrations using Landsat ETM and field spectral measurement in Taihu Lake, China. *Int J Remote Sens* 26(13):2779–2795. <https://doi.org/10.1080/01431160512331326648>
- Pavelsky TM, Smith LC (2009) Remote sensing of suspended sediment concentration, flow velocity, and lake recharge in the Peace-Athabasca Delta, Canada. *Water Resources Research*, 45(11), art. no. W11417. <https://doi.org/10.1029/2008WR007424>
- Roy, D. P., Wulder, M. A., Loveland, T. R., Woodcock, C. E., Allen, R. G., Anderson, M. C., ... Zhu, Z. (2014). Remote sensing of environment Landsat-8: science and product vision for terrestrial global change research. *Remote Sens Environ*, 145:154–172. <https://doi.org/10.1016/j.rse.2014.02.001>
- Sosa-Avalos R, Gaxiola-castro G, Olivós-Ortiz A, Silva-Iñiguez L (2013) Nutrientes inorgánicos y producción del fitoplancton en una laguna costera subtropical de México. *Rev Biol Mar Oceanogr* 48(1):143–154. <https://doi.org/10.4067/S0718-19572013000100012>
- Theologou I, Patelaki M, Karantzalos K (2015) Can single empirical algorithms accurately predict inland shallow water quality status from high resolution, multi-sensor, multi-temporal satellite data? *ISPRS-Int Arch Photogramm Remote Sens Spat Inf Sci XL-7-W3(1):1511–1516*. <https://doi.org/10.5194/isprsarchives-XL-7-W3-1511-2015>
- Uusitalo R, Yli-Halla M, Turtola E (2000) Suspended soil as a source of potentially bioavailable phosphorus in surface runoff waters from clay soils. *Water Res* 34(9):2477–2482. [https://doi.org/10.1016/S0043-1354\(99\)00419-4](https://doi.org/10.1016/S0043-1354(99)00419-4)
- Wu G, de Leeuw J, Skidmore AK, Liu Y, Prins HHT (2009) Performance of Landsat TM in ship detection in turbid waters. *Int J Appl Earth Obs Geoinf* 11(1):54–61. <https://doi.org/10.1016/j.jag.2008.07.001>
- Wu C, Wu J, Qi J, Zhang L, Huang H, Lou L, Chen Y (2010) Empirical estimation of total phosphorus concentration in the mainstream of the Qiantang River in China using Landsat TM data. *Int J Remote Sens* 31(9):2309–2324. <https://doi.org/10.1080/01431160902973873>
- Yacobi YZ, Moses WJ, Kaganovsky S, Sulimani B, Leavitt BC, Gitelson AA (2011) NIR-red reflectance-based algorithms for chlorophyll-*a* estimation in mesotrophic inland and coastal waters: Lake Kinneret case study. *Water Res* 45(7):2428–2436. <https://doi.org/10.1016/j.watres.2011.02.002>
- Yunus AP, Dou J, Sravanthi N (2015) Remote sensing of chlorophyll-*a* as a measure of red tide in Tokyo Bay using hotspot analysis. *Remote Sens Appl: Soc Environ* 2:11–25. <https://doi.org/10.1016/j.rsase.2015.09.002>
- Zhang, Y., Zhang, Y., Zha, Y., Shi, K., Zhou, Y., & Wang, M. (2015). [Remote sensing estimation of total suspended matter concentration in Xin'anjiang Reservoir using Landsat 8 data]. *Huan Jing Ke Xue=Huanjing Kexue*, 36(1), 56–63. Retrieved from <http://www.ncbi.nlm.nih.gov/pubmed/25898647>
- Zheng Z, Li Y, Guo Y, Xu Y, Liu G, Du C (2015) Landsat-based long-term monitoring of total suspended matter concentration pattern change in the wet season for Dongting Lake, China. *Remote Sens* 7(10):13975–13999. <https://doi.org/10.3390/rs71013975>